Advances in River Sediment Research – Fukuoka et al. (eds)
© 2013 Taylor & Francis Group, London, ISBN 978-1-138-00062-9

Study of flood flow and gravel riverbed variation analysis in the Satsunai river

K. Osada
Anan National College of Technology, Tokushima, Japan

S. Fukuoka
Research and Development Initiative, Chuo University, Tokyo, Japan

H. Ohgushi
Obihiro River Office, Hokkaido Development Bureau, Hokkaido, Japan

ABSTRACT: In the Satsunai river with gravel-bed, stones and gravels have moved violently during floods and severe bed scouring and bank erosion occurred. To clarify flow and sediment transport during a flood is important to design a stable longitudinal and cross-sectional form. The authors have developed a new method of two-dimensional riverbed variation analysis focused on bed surface unevenness and the mechanism of sediment transport in gravel-bed rivers. We applied the new model and the conventional model to riverbed variation of 2011 flood whose data of water surface profiles were observed in detail. We showed that the new model is a useful method for flood flows and riverbed variation in the Satsunai river with gravel-bed.

1 INTRODUCTION

In the Satsunai river with steep slope of the Tokachi river system, stones and gravels are moved violently during floods. Figure 1 shows channel changes over-time from 1971 average bed elevation. Figure 2 shows cross-sectional form in 15 km and 19.2 km section. Channel form around 1971 was wide and shallow. Many places of the main channel abutted on a river bank, because the alignment of the main channel meandered greatly. A series of dikes have been constructed from 1978 for the bank protection of the main channel. But, the main channel cross sectional form has transformed in narrow and deep shape. When a large-scale flood happened, it is likely that severe erosion of flood plain and levee would occur. To clarify flow and bed variation during a flood is important to design a stable longitudinal and cross-sectional form in the Satsunai river.

We develop a new model of two-dimensional riverbed variation focused on bed surface unevenness

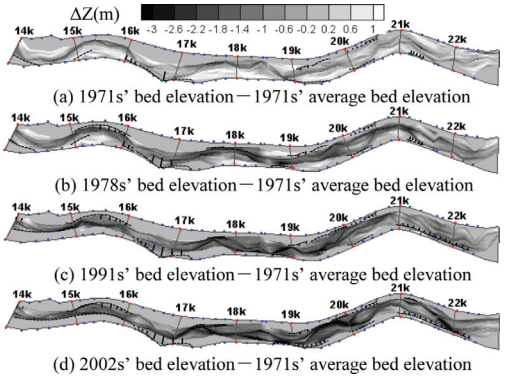

Figure 1. Channel change from 1971s' average bed elevation (Dotted line: bank revetment, Black line: dike).

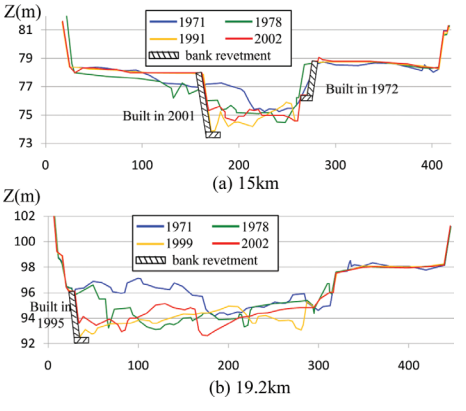

Figure 2. Transition of riverbed cross-sectional form.

in gravel-bed rivers. In this model, to take account for the bed surface unevenness, we calculate heights of each sediment size group on the bed surface. Moreover, sediment discharge in gravel-bed rivers is calculated by pick-up rate from the bed, deposit rate to the bed and particle moving velocity. In this study, we applied the authors' model to 2011 flood for the check of validation, and compared it with the conventional model which consists of Hiranos' sediment continuity equation (Hirano 1971) and Asida and Michiue sediment load equation (Ashida & Michiue 1972).

2 TWO-DIMENSIONAL MODEL OF RIVERBED VARIATION ANALYSIS IN GRAVEL-BED RIVERS

2.1 *Field investigation of bed surface unevenness*

The authors (Osada & Fukuoka 2008, 2010) expressed a height of each particle size by calculated average height of each particle size $\overline{Z_{Pk}}$ as shown in Figure 3(a). However, we see to have various heights in the same size group such as particles A and B in Figure 3(a). The differences of these heights make the bed surface unevenness and affect the amount of pick up and deposition. Thus, the field investigation was necessary to elucidate the height distributions of each particle size f_{zk} based on the average heights of each particle size $\overline{Z_{Pk}}$ as shown in Figure 3(b).

The field investigation was conducted in the field-experimental channel in the Jyoganji river (Maeshima et al. 2011). Figure 4 shows a plan view and initial cross-sectional form of the field-experimental channel. The channel is 190 m long, 8 m wide and 1:130 bed gradient. The experiment was carried out in steady flow conditions (Case 1~Case 4). The investigation was conducted on the bed surface after Case 4. No. 0 and No. 16 sections in straight reach were chosen as the investigation sections to eliminate

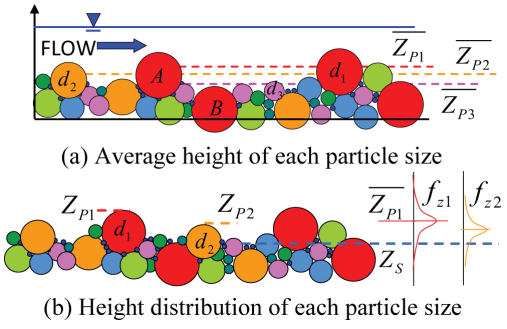

Figure 3. Relation between average height and height distribution of each particle size.

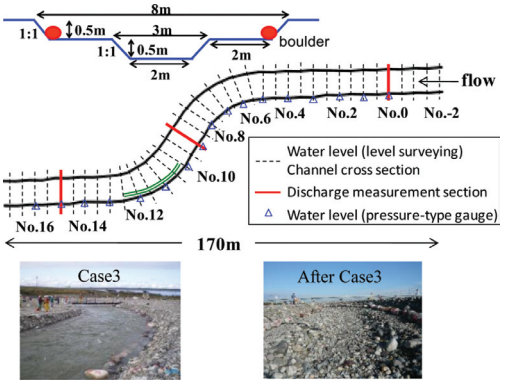

Figure 4. Plan view and initial cross sectional form of the field experimental channel.

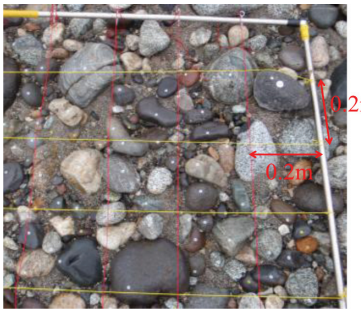

Figure 5. Bed situation of investigation site.

direct influences of the channel meander and bank slope. Numbered seals were affixed on stones and gravel as shown in Figure 5, and heights of each particle Z_{Pk} were measured by surveying. Height of a surface Z_S is also measured to determine a base level of the bed. Each particle size was estimated by the image analysis.

Figure 6 shows observed height distributions of 3 categories in particle size (d < 40 mm, 40 mm < d < 75 mm, 75 mm < d). These profiles are close to the normal distribution curve, and so equation (1) was used for estimating each particle size distribution.

$$f(z') = \frac{1}{\sqrt{2\pi}\sigma_k}\exp\left(-\frac{z'^2}{2\sigma_k^2}\right), \quad z' = \frac{Z_{Pk} - \overline{Z_{Pk}}}{\overline{Z_{Pk}} - Z_s} \quad (1)$$

Figure 7 shows observed height distributions and normal distribution curves of equation (1). Figure 8 shows the relation between particle size and standard deviation of normal distribution curves shown in Figure 5. Where d_m = mean particle diameter. This relation is approximated by equation (2).

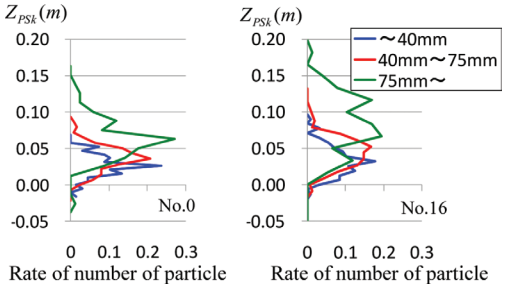

Figure 6. Observed height distributions of each particle size.

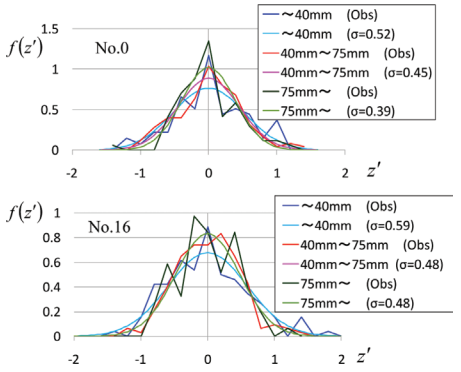

Figure 7. Approximated normal distribution curves.

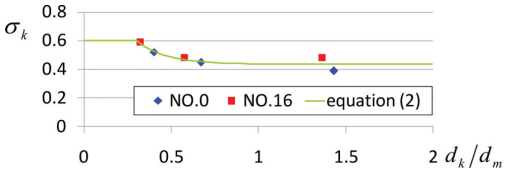

Figure 8. Relation between standard deviation and particle size.

$$\sigma_k = \min\left\{0.435 + \exp\left(-6\frac{d_k}{d_m}\right), 0.6\right\} \tag{2}$$

Maximum value of the standard deviation is assumed to be 0.6 because the value of standard deviation do not become larger than 0.6. Equation (2) is used for estimating the bed surface unevenness in the new model.

2.2 *2-D riverbed variation analysis method*

Figure 9 illustrates sediment transport mechanism resulting from bed surface unevenness in gravel-bed rivers. Figure 10 shows a procedure of the new two-dimensional riverbed variation analysis. The model is composed of unsteady two-dimensional flood flow analysis and two-dimensional riverbed variation analysis.

2.2.1 *Unsteady 2-D flood flow analysis*

The continuity and momentum equations of unsteady two-dimensional flood flow analysis are as follows:

$$\frac{\partial}{\partial t}\left(\frac{h}{J}\right)+\frac{\partial}{\partial \xi}\left(\frac{q^{\xi}}{J}\right)+\frac{\partial}{\partial \eta}\left(\frac{q^{\eta}}{J}\right)=0 \tag{3}$$

$$\begin{aligned}&\frac{\partial}{\partial t}\left(\frac{q^{\xi}}{J}\right)+\frac{\partial}{\partial \xi}\left(\frac{u^{\xi}q^{\xi}}{J}\right)+\frac{\partial}{\partial \eta}\left(\frac{u^{\eta}q^{\xi}}{J}\right)\\&-\frac{q_x}{J}\left(u^{\xi}\frac{\partial \xi_x}{\partial \xi}+u^{\eta}\frac{\partial \xi_x}{\partial \eta}\right)-\frac{q_y}{J}\left(u^{\xi}\frac{\partial \xi_y}{\partial \xi}+u^{\eta}\frac{\partial \xi_y}{\partial \eta}\right)\\&=-gh\left(\frac{\xi_x^2+\xi_y^2}{J}\frac{\partial H}{\partial \xi}+\frac{\xi_x\eta_x+\xi_y\eta_y}{J}\frac{\partial H}{\partial \eta}\right)\\&-\frac{F_{D90}^{\xi}}{\rho J}+D^{\xi}\end{aligned} \tag{4}$$

$$\begin{aligned}&\frac{\partial}{\partial t}\left(\frac{q^{\eta}}{J}\right)+\frac{\partial}{\partial \xi}\left(\frac{u^{\xi}q^{\eta}}{J}\right)+\frac{\partial}{\partial \eta}\left(\frac{u^{\eta}q^{\eta}}{J}\right)\\&-\frac{q_x}{J}\left(u^{\xi}\frac{\partial \eta_x}{\partial \xi}+u^{\eta}\frac{\partial \eta_x}{\partial \eta}\right)-\frac{q_y}{J}\left(u^{\xi}\frac{\partial \eta_y}{\partial \xi}+u^{\eta}\frac{\partial \eta_y}{\partial \eta}\right)\\&=-gh\left(\frac{\xi_x\eta_x+\xi_y\eta_y}{J}\frac{\partial H}{\partial \xi}+\frac{\eta_x^2+\eta_y^2}{J}\frac{\partial H}{\partial \eta}\right)\\&-\frac{F_{D90}^{\eta}}{\rho J}+D^{\eta}\end{aligned} \tag{5}$$

where h = flow depth; q^{ξ}, q^{η} = contravariant components of discharge fluxes; u^{ξ}, u^{η} = contravariant components of velocity vectors; H = water level ($h+\overline{Z_B}$); $\overline{Z_B}$ = Average of riverbed elevation J = Jacobian; $\xi_x, \xi_y, \eta_x, \eta_y$ = metrics; D^{ξ}, D^{η} = the terms of depth-averaged Reynolds stress.

Form resistance of large stones is dominant to bed resistance. The equations for evaluating bed resistance are developed by using form resistance of diameter d_{90} on the bed surface as follows:

$$F_{D90}^{\xi}=\xi_x F_x+\xi_y F_y, \quad F_{D90}^{\eta}=\eta_x F_x+\eta_y F_y \tag{6}$$

$$\begin{pmatrix}F_x\\F_y\end{pmatrix}=N_{D90}\frac{\varepsilon_{D90}}{2}\rho C_D A_{D90}u_{D90}^2\frac{1}{\sqrt{u_x^2+u_y^2}}\begin{pmatrix}u_x\\u_y\end{pmatrix} \tag{7}$$

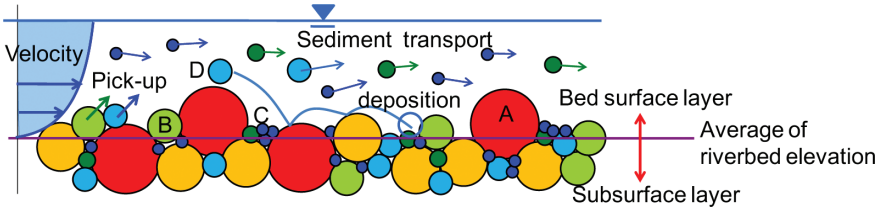

Figure 9. Relationship between bed surface, flow and sediment transport.

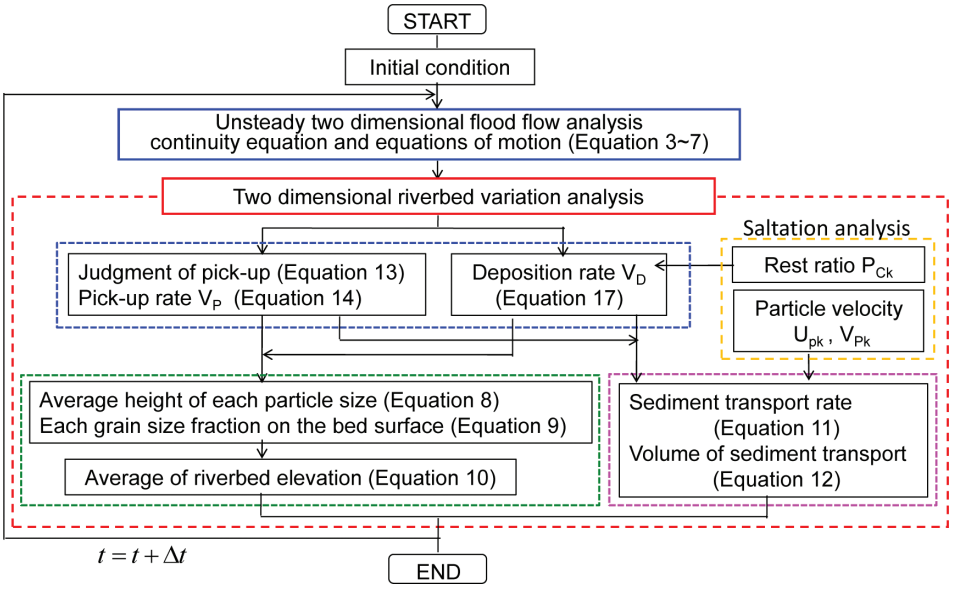

Figure 10. Procedure of the two-dimensional riverbed variation analysis.

where F_x, F_y = x- and y-components of form resistance of d_{90}; N_{D90} = number of d_{90} on the bed surface defined as $N_{D90} = 0.2/\alpha_2\, d_{90}^2$; ε_{D90} = shielding coefficient of d_{90} (=0.48); ρ = water density; C_D = drag coefficient (=1.0); A_{D90} = projected area of d_{90}; u_{D90} = flow velocity acting on d_{90} which is determined by the logarithmic velocity distribution.

2.2.2 *Average height and fraction of each size on the bed surface*

Average height of each particle size $\overline{Z_{Pk}}$ is estimated by using pick-up rate V_{Pk}, deposit rate V_{Dk} and each particle size fraction on the bed surface P_k.

$$\frac{\partial \overline{Z_{Pi,j,k}}}{\partial t} = -\frac{\alpha_2}{\alpha_3}\frac{\left(V_{Pi,j,k} - V_{Di,j,k}\right)}{P_{i,j,k}} \tag{8}$$

where subscript i, j indicates the computational grid number; α_2, α_3 = 2-D and 3-D shape factors of the particles ($=\pi/4, \pi/6$). Each particle size fraction on the bed surface P_k is calculated by using pick-up rate V_{Pk} and deposit rate V_{Dk}.

$$\frac{\partial P_{i,j,k}}{\partial t} = -\frac{\alpha_2}{\alpha_3}\frac{\left(V_{Pi,j,k} - V_{Di,j,k}\right)}{d_k} + P_{0i,j,k}\sum_{k=1}^{nk}\frac{\alpha_2}{\alpha_3}\frac{\left(V'_{i,j,k}\right)}{d_k} \tag{9}$$

$$V'_{i,j,k} = \begin{cases} V_{Pi,j,k} - V_{Di,j,k}, & V_{Pi,j,k} > V_{Di,j,k} \\ 0 \qquad\qquad\quad , & V_{Pi,j,k} \le V_{Di,j,k} \end{cases}$$

where $P_{0i,j,k}$ = each particle size fraction in the subsurface layer. Average of riverbed elevation $\overline{Z_B}$ is defined as equation (10).

$$\overline{Z_{Bi,j}} = \sum_{k=1}^{nk}\left(P_{i,j,k}\cdot\overline{Z_{Pi,j,k}}\right) - \frac{d_{mi,j}}{2} \tag{10}$$

The first term on the right side represents the average particle height in the computational grid, and the second term is radius of the mean particle diameter.

2.2.3 *Estimation method of sediment transport rate*

Sediment transport rate of each particle size is evaluated by the product of the volume of sediment transport V_{mk} and particle velocity u_{pk}.

$$q_{B\xi i,j,k} = V_{m\,i0,j,k}\,\overline{u_{p\xi\,i,j,k}}$$
$$q_{B\eta i,j,k} = V_{m\,i,j0,k}\,\overline{u_{p\eta\,i,j,k}} \tag{11}$$

Volume of sediment transport per unit of area V_{mk} is calculated by a balance of sediment transport rate and difference between pick-up rate and deposit rate.

$$\frac{\partial V_{mi,j,k}}{\partial t} + \frac{\partial q_{B\xi i,j,k}}{\partial \xi} + \frac{\partial q_{B\eta i,j,k}}{\partial \eta} = V_{Pi,j,k} - V_{Di,j,k} \tag{12}$$

Particle velocities of each particle size $\overline{u_{P\xi k}}$, $\overline{u_{P\eta k}}$ are estimated by saltation analysis using the particle equation of motion as shown in Figure 11. Bed surface is formed by the mean particle diameter considering the longitudinal and cross-sectional bed gradient. Coefficient of restitution (=0.65) is used for calculating the collision with the bed materials.

2.2.4 *Calculation method of pick-up rate*

The particles located at high position such as A particle in Figure 9 have a high probability of pick-up from the bed. On the other hand, particles such as B and C particles cannot be picked up from the bed by the effect of larger stones. Pick-up equation was developed by considering these mechanisms.

First, pick-up critical elevation of each particle size is estimated by balance-of-moment equation (equation (13)). Pick-up critical elevation is defined as the elevation of $\beta = 1$ as shown in Figure 12, it is calculated by shifting particle height.

$$\beta_{i,j,k} = \frac{\frac{\alpha_{zk}}{2}\rho C_D \varepsilon_a \alpha_2 d_k^2 u_{fk}^2 + \frac{\alpha_{xk}}{2}\rho C_L \varepsilon_a \alpha_2 d_k^2 u_{fk}^2}{\alpha_{xk}\cdot(\rho_s - \rho) g \alpha_3 d_k^3} \tag{13}$$

($\beta_k \geq 1.0$:Pick up, $\beta_k < 1.0$:No pick up)

$$\alpha_{xk} = \frac{d_k}{2}\sin\theta_k, \quad \alpha_{zk} = \frac{d_k}{2}\cos\theta_k$$

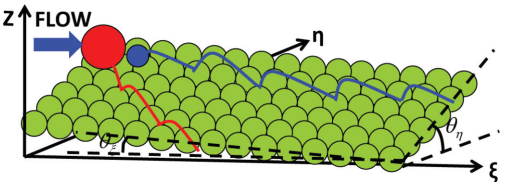

Figure 11. Concept of the saltation analysis.

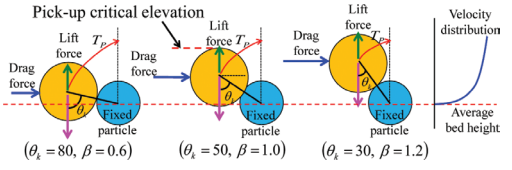

Figure 12. Pick-up critical elevation.

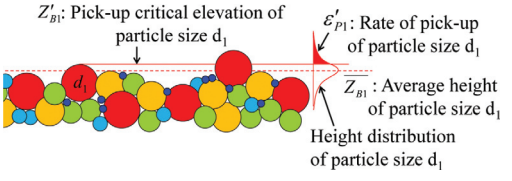

Figure 13. Rate of pick-up.

where ε_a = projected area coefficient (=0.7); C_L = lift coefficient (=0.85); ρ_s = particle density; u_{fk} = the velocity acting on the particle; θ_k = angle of pick up from the bed. Next, pick-up rate is determined by equation (14), when the sediment particle is judged to move by equation (13).

$$V_{Pi,j,k} = \varepsilon'_{P\,i,j,k}\,\varepsilon_{wsi,j,k}\,\frac{N_{Pi,j,k}\,\alpha_3 d_k^3}{T_{Pi,j,k}} \tag{14}$$

where ε'_{Pk} = rate of pick up calculated by height distribution; ε_{wsk} = rate of pick up controlled by the shielding effect of large materials; N_{Pk} = number of particles of each particle size on the bed surface ($= P_k / \alpha_2 d_k^2$); T_{Pk} = time required for pick up from the bed.

Rate of pick-up of each particle size ε'_{Pk} is defined by a ratio above the pick-up critical elevation as shown in Figure 13, and it is calcurated by equation (15).

$$\varepsilon'_{Pi,j,k} = \varepsilon_r \int_{Z'_{Bk}}^{\infty} \frac{1}{\sqrt{2\pi}\sigma_{i,j,k}} \exp\left(-\frac{z^2}{2\sigma_{i,j,k}^2}\right) dz \tag{15}$$

where ε_r: coefficient in consideration of a delay of the time of the pick-up by the vibrancy.

ε_{wsk} is estimated by equation (16).

$$\varepsilon_{wsk} = 1 - \max\left\{ \sum_{k'=1}^{nk'} \left(\frac{P_{wk,k'}}{\alpha_2 d_{k'}^2} A_{wk'} \right) + \sum_{k'=1}^{nk'} \left(\frac{P_{sk,k'}}{\alpha_2 d_{k'}^2} A_{sk'} \right), 1.0 \right\} \quad (16)$$

where subscript k' indicates the particle size of $d_{k'} \geq d_m$ and $d_{k'} \geq d_k$; $P_{wk,k'}, P_{sk,k'}$ = respective rates of particle k' located in a wake zone and at the front of the particle k; and $A_{wk'}, A_{sk'}$ = control areas of pick up by shielding effects shown in Figure 14 ($\alpha_S = 1$, $\alpha_W = 1$).

2.2.5 *Calculation method of deposit rate*

The amount of deposition on the bed per unit time V_{Dk} is calculated by equation (17).

$$V_{Di,j,k} = P_{Ci,j,k} V_{mi,j,k} \quad (17)$$

where, P_{Ck} is the rest ratio of each particle estimated by saltation analysis. As shown in Figure 15, saltation analysis is conducted on the bed formed so as to coincide approximately with particle size distribution and height distributions, and moving period t_s is estimated by this saltation analysis. The rest ratio P_{Ck} is calculated by equation (18) using the moving period.

$$P_{Ci,j,k} = \int_0^1 \frac{1}{t_{Si,j,k}} \exp\left(-\frac{t}{t_{Si,j,k}} \right) dt \quad (18)$$

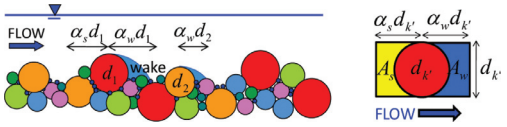

Figure 14. Shielding effect by large stones.

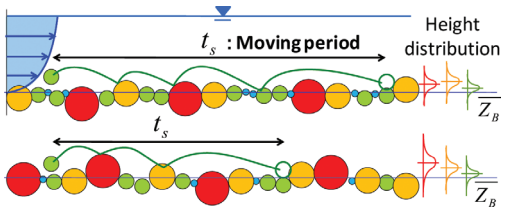

Figure 15. Saltation analysis for estimated moving period.

3 APPLICATION TO 2011 FLOOD

3.1 *Analysis condition*

We applied the new model and conventional model (Egiazaroff 1965, Hirano 1971, Ashida & Michiue 1972) to the Satsunai river. The analysis was performed from 14.0 km to 23.0 km as shown in Figure 16. The results of these models were compared to the observed results of 2011 flood. Figure 16 shows observation stations of water levels. Water level gauges of simple pressure type were installed at 6 points (No. 1~No. 6) in addition to the existing 2 observation stations. The upstream boundary condition was given observed water level hydrographs at Daini-ohkawabashi (20.7 km section) and No. 6, and the downstream boundary condition observed water level hydrographs at Nantaibashi (15.0 km section).

Figure 17 shows air photographs taken before and after 2011 flood. They show longitudinal channel variations during the flood. To introduce enough the initial riverbed form for the analysis is important for explaining these longitudinal channel variations. The reproduction of initial riverbed form was made by referencing air photographs.

Figure 18 shows measured particle size distributions in the Satsunai river. These particle size distributions were measured by removing stones more than 0.15 m. Thus particle size distribution of black line shown in Figure 18 which was corrected was used for the analysis. Five particle sizes (250 mm, 120 mm, 50 mm, 10 mm, 2 mm) were used in the calculation.

3.2 *Result of analysis and consideration*

3.2.1 *On flood flow*

Figure 19 and Figure 20 show comparison with observed and calculated water level hydrographs and discharge hydrographs by using the conventional model. The Manning's roughness coefficient

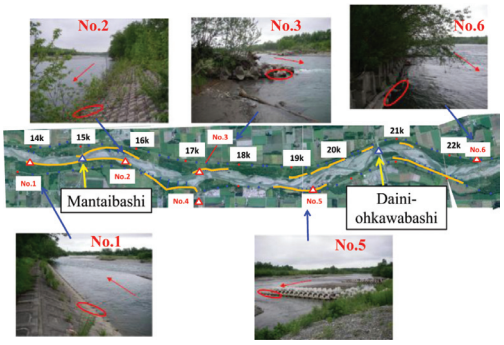

Figure 16. Observation stations of water levels.

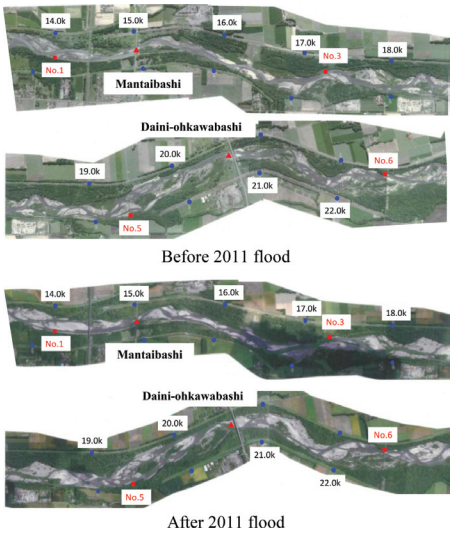

Figure 17. Channel variation during 2011 flood.

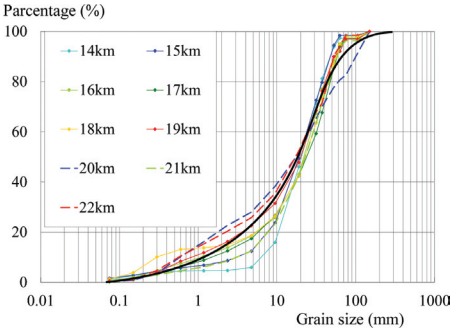

Figure 18. Initial grain size distributions for calculation.

n = 0.03 was given to reproduce water level and discharge for the conventional model. Figure 19 shows the calculated results at No. 6 and Daini-ohkawabashi were generally reproduced observed water level hydrographs. However, observed water level hydrographs of the other points (No. 5, No. 3, No. 1 and Nantaibashi) cannot be explained by the conventional model. The riverbed variations appear to affect the water surface profiles. But, as shown below, the result of riverbed variation by using the conventional model could not reproduce observed riverbed variation, so that calculated water level hydrographs were not reproduced observed results. Calculated discharge hydrographs were estimated excessively in the falling period of the flood compared to the observed results.

Figure 21 and Figure 22 show the results of the authors' model. Figure 21 shows the calculated water level hydrographs at No. 6, No. 5 and Nantaibashi were reproduced observed results to a certain level. However, calculated water level hydrographs at Daini-ohkawabasi and No. 3 were estimated fairly low as compared to the observed results. As shown below, the authors' model cannot explain enough bank erosion and channel variation of 2011 flood, and thus cannot reproduce water level hydrographs. Figure 22 shows that calculated discharge hydrographs agreed well observed results. Figure 23 shows calculated results of depth and velocity distribution at the time of the peak discharge in 2011 flood. However, the depth is deep and velocity is fast locally due to flow concentration to narrow and deep parts in the main channel.

3.2.2 *Sediment transport and riverbed variation*

Figure 24 shows the comparison between calculated and observed riverbed variation by 2011 flood. Figure 25 and Figure 26 show the calculated

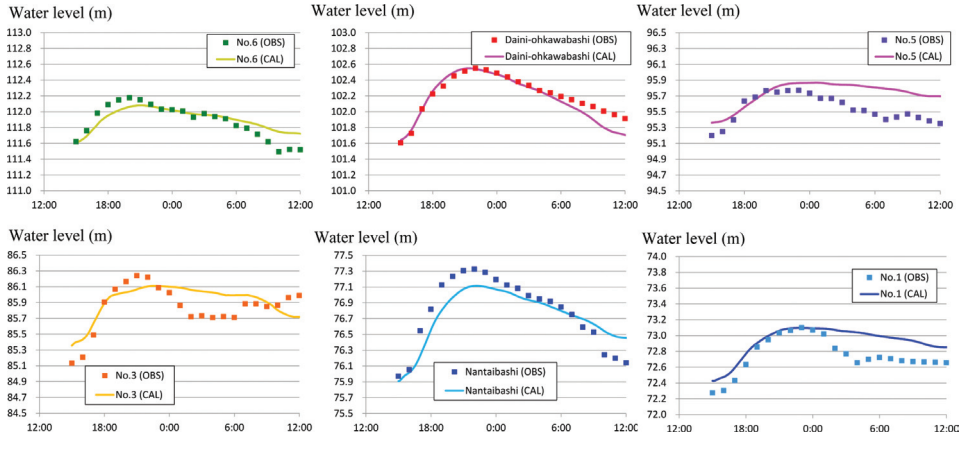

Figure 19. Comparison between observed and calculated water level hydrograph (Conventional model).

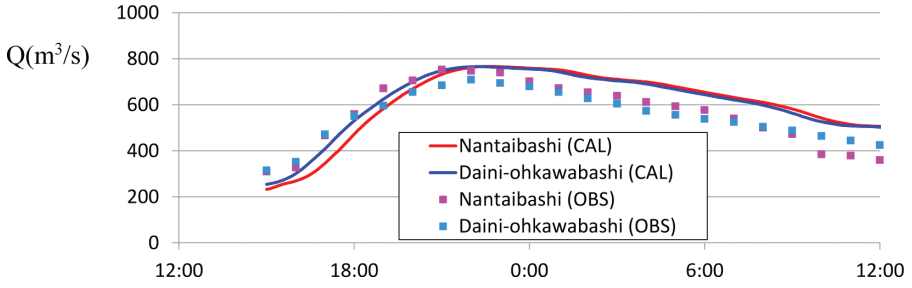

Figure 20. Comparison between observed and calculated discharge hydrograph (Conventional model).

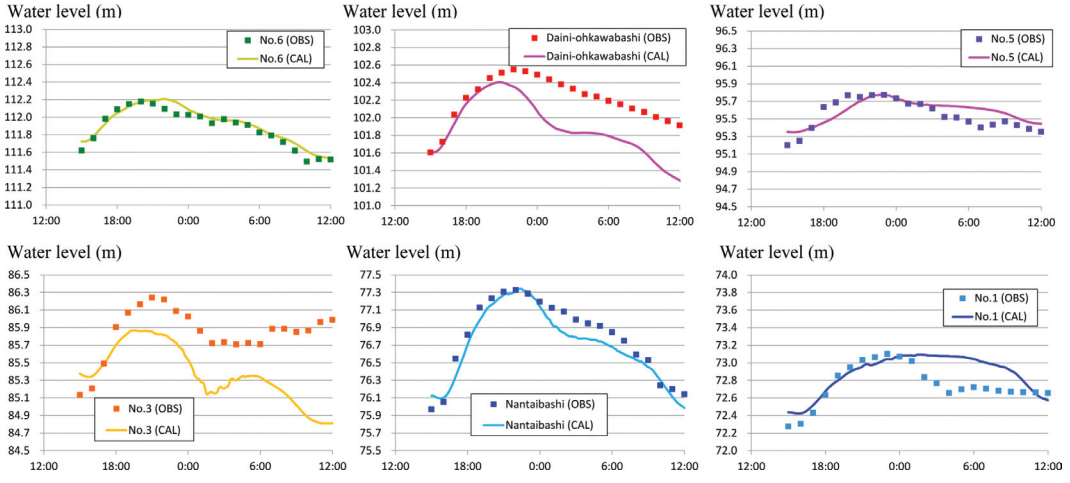

Figure 21. Comparison between observed and calculated water level hydrograph (Authors' model).

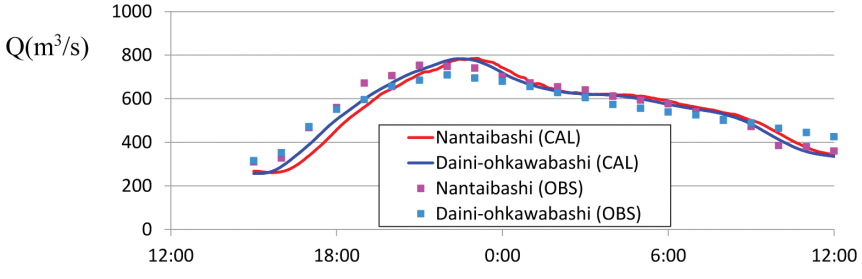

Figure 22. Comparison between observed and calculated discharge hydrograph (Authors' model).

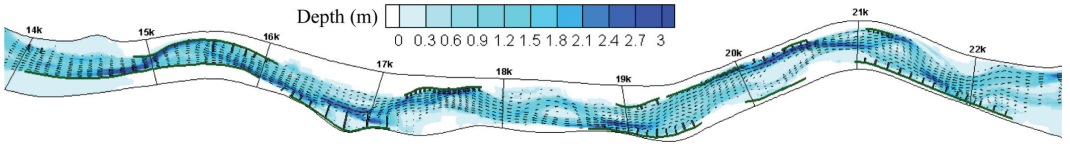

Figure 23. Depth and velocity distribution at time of the peak discharge.

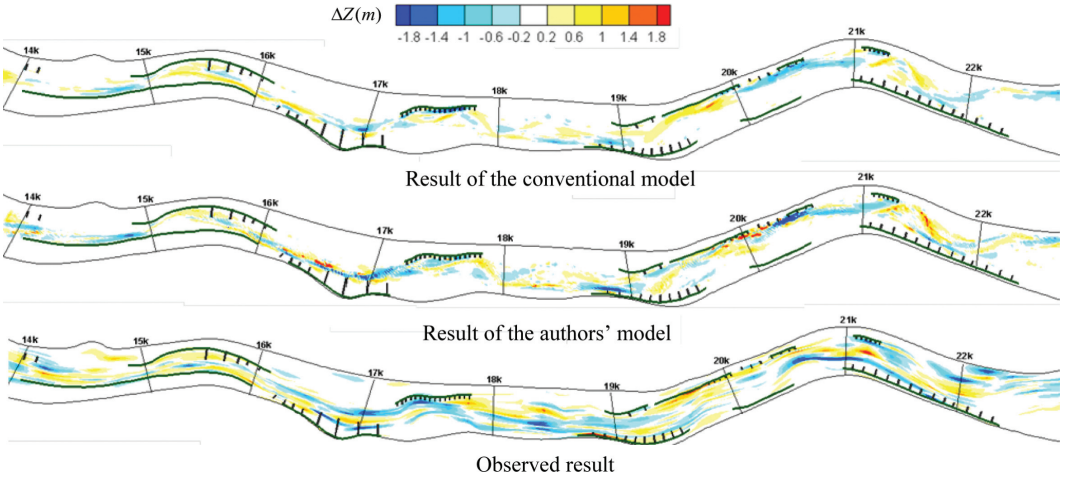

Figure 24. Comparison between calculated and observed riverbed variation.

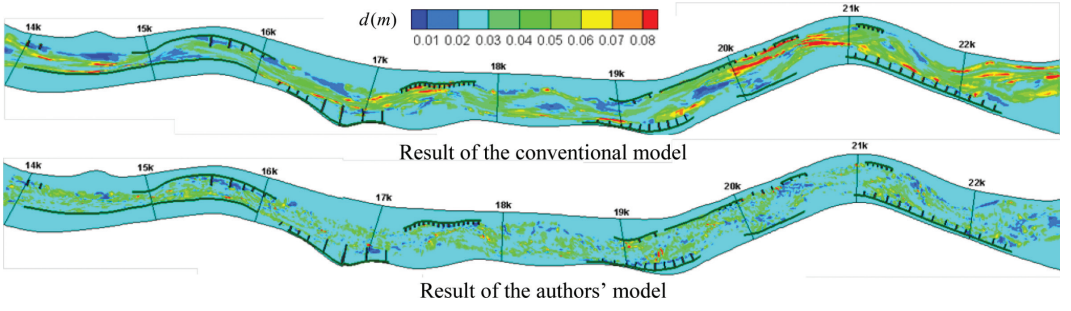

Figure 25. Calculated result of D60.

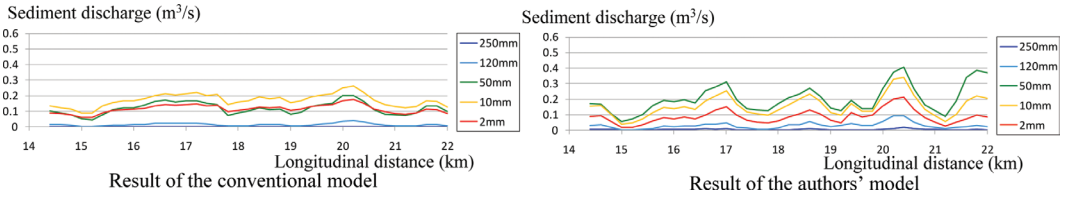

Figure 26. Sediment discharge of each grain size at time of the peak discharge.

results of D60 spatial distributions and sediment discharge of each particle size.

First, the authors' model result of riverbed variation was under estimated longitudinally compared to observed riverbed variation as shown in Figure 24. The data of sediment discharge by the conventional model indicate extensive transport of gravel size materials as 10 mm, whereas larger size materials were hardly transported. The calculated sediment discharge and riverbed variation could not estimate actual phenomena, so that calculated results of water level hydrograph could not also explain observed results. The conventional model which cannot reproduce sediment transport of larger size materials does not appear to explain riverbed variation in the gravel-bed rivers.

On the other hand, riverbed variation by authors' model was larger than the result of the conventional model as shown in Figure 24. However, the authors' model cannot reproduce enough

bank erosion such as around Daini-ohkawabashi (20.7 km) and bed scouring by the channel variation such as around No. 3 observation point, because a mechanism of bank erosions are not considered. Figure 26 shows that large gravels and cobbles were transported activity by using the authors' model, and its total transported amount was larger than those of the conventional model.

The authors' model cannot reproduce calculated water level hydrograph in several points because bank erosion and channel variation around the observation point cannot explain enough. However, the authors' model is capable of explaining sediment transport rate and riverbed variation in the Satsunai river compared to the conventional model.

4 CONCLUSION

We developed the new model of two-dimensional riverbed variation focused on bed surface unevenness and the mechanism of sediment transport in gravel-bed rivers. We conducted the check of validation of the authors' new model and compared with the conventional model by 2011 Satsunai river flood.

The conventional model gives considerably less results than observed results of sediment transport rate and riverbed variation. The conventional model revealed to be insufficient to explain sediment transport rate and riverbed variation in gravel-bed rivers. On the other hand, the authors' model gives better sediment transport of large gravel and cobble size groups and riverbed variation than the conventional model. This showed that the authors' model was a useful method for sediment transport and riverbed variation in the Satsunai river with gravel-bed.

REFERENCES

Ashida, K. and Michiue, M. 1972. Study on Hydraulic Resistance and Bed-Load Transport Rate in Alluvial Streams, *Proceedings of the Japan Society of Civil Engineers*, No. 206, pp. 59–69.

Egiazaroff, I.V. 1965. Calculation of Nonuniform Sediment Concentration, *Proc. ASCE*, Vol. 91, HY4, pp. 225–247.

Hirano, M. 1971. River-Bed Degradation with Armoring, *Proceedings of the Japan Society of Civil Engineers*, No. 195, pp. 55–65.

Maeshima, T., Iwasa, M., Osada, K. and Fukuoka, S. 2011. Study on River-Bed Variation and Its Grain Size Distribution in Compound Stony-Bed River With Meandering and Straight Channel, *Annual Journal of Hydraulic Engineering*, JSCE, Vol. 55, pp. 769–774.

Osada, K. and Fukuoka, S. 2008. Development of One-dimensional Bed Variation Analysis Methods Focused on the Mechanism of Sediment Transport in Stony-Bed Rivers*, Advances in Hydro-Science and Engineering*, Vol. 8, ICHE Nagoya, Japan.

Osada, K. and Fukuoka, S. 2010. Analysis of Two-Dimensional Riverbed Variation in Channels with Stony Beds*, 11th International Symposium on River Sedimentation*, South Africa, CD-ROM.